

Raman spectra, superconductivity, and structure of Co-substituted $\text{YBa}_2\text{Cu}_3\text{O}_{7-\delta}$

M. Kakihana and L. Börjesson

Department of Physics, Chalmers University of Technology, S-412 96 Gothenburg, Sweden

S. Eriksson

Department of Inorganic Chemistry, Chalmers University of Technology, S-412 96 Gothenburg, Sweden

P. Svedlindh and P. Norling

Uppsala University, Institute of Technology, Box 534, S-751 21 Uppsala, Sweden

(Received 17 April 1989)

A systematic Raman spectroscopic investigation has been performed on $\text{YBa}_2\text{Cu}_{3-x}\text{Co}_x\text{O}_{7-\delta}$ ceramic samples of different Co content x in the interval $0 \leq x \leq 0.6$. The structure and the superconducting properties of the samples have been carefully characterized by x-ray diffraction, magnetic susceptibility, and resistivity measurements. It is found that the frequency of the axial stretching vibration of O(4) at 502 cm^{-1} decreases, the frequency of the Cu(2)-O(2),O(3) in-phase bending vibration at 440 cm^{-1} increases, and the frequency of the Cu(2)-O(2),O(3) out-of-phase bending vibration at 335 cm^{-1} remains constant for increasing Co concentration. The dependencies of the frequencies as well as of the intensities of these vibrational modes on cobalt substitution are reminiscent of the behavior of the corresponding modes for pure $\text{YBa}_2\text{Cu}_3\text{O}_{7-\delta}$ of increasing oxygen deficiency. It is proposed that the frequency of this mode is directly dependent on the free-charge carrier concentration and is sensitive to the charge balance between the chains and the planes. Moreover, the resultant changes of the vibrational modes on Co substitution provide additional evidence for the mode assignments of $\text{YBa}_2\text{Cu}_3\text{O}_{7-\delta}$.

I. INTRODUCTION

Since the discovery of high-temperature superconductivity in perovskite copper oxides^{1,2} various experimental techniques have been applied to elucidate the origin and the properties of the superconductivity in these materials. Since the classical weak-coupling phonon-mediated superconductivity seems to be ruled out in these materials by a negligible isotope shift of the transition temperature T_c , new pairing mechanisms, involving spin,^{3(a)} exciton,^{3(b)} and strong phonon-coupling,^{3(c),(d)} or even a new ground state^{3(e)} have been proposed to explain the high-temperature superconductivity.⁴ However, so far no conclusive experiments have been reported and the superconducting mechanism remains unknown. A useful and established method in superconductivity research is to investigate the effects of different kinds of isomorphic substitutions, e.g., isotope substitutions or replacements of atoms of different magnetic moment, radius, mass, and valence, on the superconductivity and its related properties. A well-known example is that the addition of paramagnetic impurities in the classical superconductors leads to a linear decrease of T_c ,⁵ which can be explained, within an extended weak-coupling BCS theory,⁶ as pair breaking induced by an interaction between the paramagnetic impurities and the conduction electrons.

The method of atomic replacement in $\text{YBa}_2\text{Cu}_3\text{O}_{7-\delta}$ has proven to give valuable insight into the superconducting properties. Replacement of Y by other rare-earth elements possessing large magnetic moments (ex-

cept Ce, Pr, and Tb) does not significantly affect the superconductivity.⁷ This implies that the rare-earth site is not involved in the superconducting mechanism since otherwise the localized magnetic moments would reduce the transition temperature. However, there is a slight increase of T_c with increasing radius of the rare-earth element, probably due to an expansion of the unit cell and an increase of density of states near the Fermi level. Furthermore, partial substitution of Ba ions by Sr and/or Ca only has minor effects on the superconducting properties of Y-Ba-Cu-O.⁸

Since different substitutions for Y and Ba in Y-Ba-Cu-O show that the superconductivity involves neither the Y site nor the Ba site, the two-dimensional Cu-O planes Cu(2)-O(2), O(3), and the Cu(1)-O(1) chains (see Fig. 1) are primarily associated with the high- T_c superconductivity. An understanding of the physical properties of the different Cu-O environments is thus essential for an explanation of the superconducting mechanism. Replacement of Cu by other transition metal ions is therefore expected to give valuable information about the significance and role of the different Cu-O layers for the superconductivity. [The Cu(2)-O(2), O(3), and Cu(1)-O(1) planes will hereafter be denoted as the CuO_2 planes and the CuO chains, respectively.]

Recently, it has been reported that 3d transition-metal substitution for Cu in Y-Ba-Cu-O causes a decrease of T_c as well as a broadening of the superconducting transition.⁹⁻¹² Interestingly, recent neutron-diffraction studies,¹³⁻¹⁶ Mössbauer,^{15,17,18} and extended x-ray-absorption

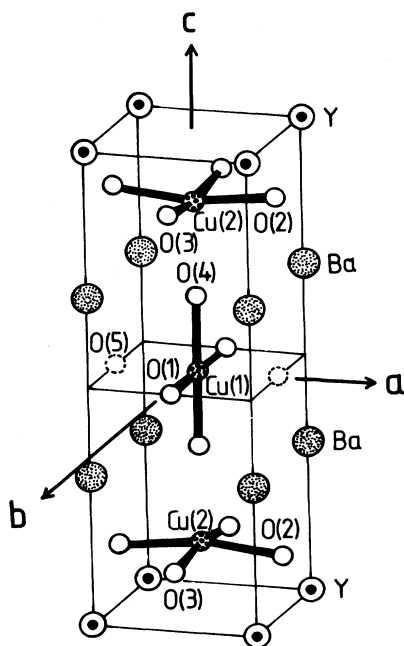


FIG. 1. Schematic structure of the orthorhombic phase of $\text{YBa}_2\text{Cu}_3\text{O}_{7-\delta}$.

fine structure¹⁹ (EXAFS) experiments demonstrate that the different 3d transition-metal ions have selective occupancies for the Cu sites in $\text{YBa}_2\text{Cu}_{3-x}\text{M}_x\text{O}_{7-\delta}$ ($M = \text{Co}, \text{Fe}, \text{Zn}, \text{Al}, \text{Ga}, \text{and Ni}$). For small concentrations of M (<5%) the trivalent Cu, Fe, Al, and Ga ions are exclusively introduced into the Cu(1) site while the divalent Ni and Zn ions preferentially occupy the Cu(2) site. At higher concentrations Fe enter both Cu(1) and Cu(2) positions. In contrast, for the Co, Zn, and Ni the same selective occupancy, as for the low- M concentration materials, continues up to their solubility limits ($x = 1.0, 0.3, \text{and } 0.3$, respectively). The different site preferences for the different ions offer the possibility to study the effect of magnetic as well as nonmagnetic ions in the CuO_2 planes and the CuO chains selectively. The reported decrease of T_c for magnetic and nonmagnetic ions shows a rather unexpected behavior, i.e., the nonmagnetic Zn gives rise to the steepest decrease of T_c with increasing impurity concentration.²⁰ Thus, magnetic pair breaking cannot be the dominant mechanism for the decrease in T_c of M substituted Y-Ba-Cu-O. Rather, it has been proposed that the local disorder induced by the metal substitution is responsible for the loss of superconductivity.²⁰ On the other hand, from recent neutron-diffraction studies of Co-substituted Y-Ba-Cu-O it is shown that T_c is correlated to bond lengths¹⁴ and that Co substitution enhances the antiferromagnetic coupling between the CuO chains and the CuO_2 planes.²¹

In this paper we report on an extensive room-temperature Raman spectroscopic investigation of carefully prepared and well-characterized $\text{YBa}_2\text{Cu}_{3-x}\text{Co}_x\text{O}_{7-\delta}$ superconductors. The samples were characterized by magnetic susceptibility, x-ray

diffraction, and resistivity measurements. The aim is to gain further insight into the superconductivity and the structure of the high- T_c superconductors from the changes of the phonon spectrum and the structure with increasing cobalt impurity content.

Raman spectroscopy has proven to be a useful tool to study copper-oxide superconductors.²² The phonon spectrum of the pure superconductors observed by Raman spectroscopy is dominated by the oxygen vibrations which are of special interest for investigating the possibility of an electron-phonon coupling as the pairing mechanism. Indeed, a distinct electron-phonon coupling has been observed for two phonon modes in Y-Ba-Cu-O, involving oxygen [O(2),O(3)] in the CuO_2 planes and Ba, as Fano interference of the phonon modes with a continuum of electronic states as well as a softening of the [O(2),O(3)] mode at T_c . Moreover, recent reports on two-magnon Raman scattering from LaSrCuO_4 and Y-Ba-Cu-O show a decrease of the two-magnon mode intensity at the superconducting transition indicating a coupling of the charge carriers to spin fluctuations.²⁷⁻³⁰ It should also be noted that Raman spectroscopy is a sensitive method to detect impurity phases owing to the small scattering cross section of the superconducting phase compared to the much stronger scattering from the semiconducting impurity phases.²²

II. EXPERIMENT

Great care was taken to produce high-quality single-phase samples to avoid traces of the strong Raman scattering from the semiconducting impurity phases. A series of samples in the $\text{YBa}_2\text{Cu}_{3-x}\text{Co}_x\text{O}_{7-\delta}$ system with $x = 0, 0.05, 0.15, 0.2, 0.3, 0.4, 0.5, \text{and } 0.6$ were prepared by a solid-state reaction of stoichiometric amounts of Y_2O_3 , CuO, BaCO_3 , and CoO (or CoCO_3), each 99.9% pure. The powders were thoroughly mixed in an agate ball mill for 30 min, and then calcined in air at 940 °C for 30 h in alumina crucibles. The black products were then reground and pressed into pellets with a diameter of 13 mm and a thickness of ~ 2 mm. The pellets were then heated to 900 °C for 15 h, cooled to 400 °C and kept there for about 20 h, then allowed to cool to room temperature in the furnace. The treatment at 400 °C and the cooling down to room temperature were always made in an O_2 atmosphere.

The sample purity as well as the structural changes were investigated as a function of dopant concentration by means of x-ray powder diffraction. The data were collected on Guinier cameras ($\text{CuK}\alpha_1$ radiation) and Si was used as an internal standard. The films were evaluated with a photoscanning system in combination with computer programs for indexing and unit cell refinement.

Room-temperature Raman spectra were recorded with a standard apparatus consisting of a double monochromator (Spex model 1403), a cooled photomultiplier (RCA 31034-76), and an argon-ion laser. For excitation the laser line at 5145 Å was used with a power of approximately 150 mW at the sample surface. All spectra were recorded in VV polarization and backscattering geometry. In order to avoid excessive heating of the sam-

ple, the laser beam was focused to a line image on the sample surface using a cylindrical lens. The slit widths were set to give a resolution of about 8 cm^{-1} .

III. RESULTS

A. Resistivity measurements

The results of the resistivity measurements are shown in Fig. 2. All resistivity curves are normalized to their respective room-temperature resistivity values. The samples with $x \leq 0.2$ show metallic resistance down to the transition temperature. The transitions for these samples are sharp ($\Delta T_c \approx 3 \text{ K}$). For the samples with $x \geq 0.3$ there are upward curvatures of the resistivity which either persist down to the transition temperature ($x = 0.3$) or to 4 K for the samples for which no zero resistance was observed ($x = 0.4, 0.5, 0.6$). The transition width is broader ($\Delta T_c \approx 6 \text{ K}$) for the samples which show upward bends of the resistivity curve. In Fig. 3 the transition temperature (midpoint) is presented as a function of Co concentration. The results indicate an almost linear decrease of T_c between $x = 0.15$ and $x = 0.4$ and a plateau-like behavior between $x = 0$ and $x = 0.1$. The reported results of other authors^{15,31,32} are also included in Fig. 3 as a comparison. Although the different results follow about the same trend there is a large scatter of the T_c results, which is probably due to a variation of the oxygen content and/or the presence of impurities in the different samples.

B. Magnetic measurements

In order to further characterize the superconducting properties, magnetization measurements have been performed on samples with $x \leq 0.2$ using a SQUID magnetometer in the temperature range 30–100 K. Both the zero-field-cooled (ZFC) and the field-cooled (FC) magne-

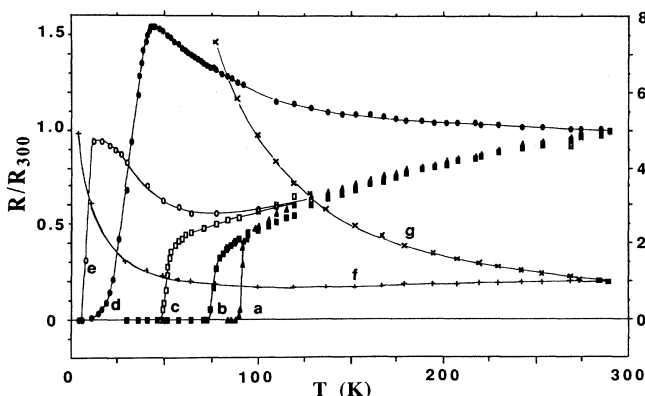


FIG. 2. Resistivity vs temperature for the different $\text{YBa}_2\text{Cu}_{3-x}\text{Co}_x\text{O}_{7-\delta}$ samples. Curve a, $x = 0.05$; curve b, $x = 0.15$; curve c, $x = 0.2$; curve d, $x = 0.3$; curve e, $x = 0.4$; curve f, $x = 0.5$; curve g, $x = 0.6$. The resistivity curves are normalized by their respective value at room temperature. Left-hand scale, curves a–e; right-hand scale, curves f and g.

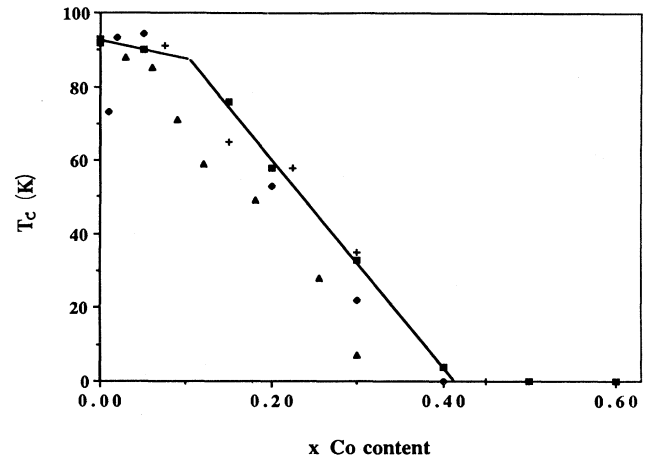


FIG. 3. T_c vs a function of Co concentration in $\text{YBa}_2\text{Cu}_{3-x}\text{Co}_x\text{O}_{7-\delta}$. (■) present results; (Δ), (\blacklozenge), and (+) results of Refs. 32, 31, and 15, respectively. The solid line is a guide to the eye through the present results.

tizations were studied. In the ZFC measurements the sample is cooled in zero field to a low temperature below T_c , where a small magnetic field (1 G) is applied. The magnetization is then probed as a function of temperature as the sample is slowly warmed up through T_c . In the FC procedure, where the Meissner expulsion is measured, the sample is cooled in a small applied field (1 G) while monitoring the magnetization. The results on all samples ($x = 0, 0.05, 0.15, 0.2$) show sharp transitions (half width $\Delta T_c \leq 5 \text{ K}$) with no indications of two-phase character or impurity phases. The midpoints of the FC transitions are typically 1–2 K higher than for the ZFC transitions and are in good agreement with the midpoints of the corresponding resistive transitions. Furthermore, the FC magnetization values are roughly 10–15% of the corresponding ZFC values. This is a common observation made in experiments on high- T_c materials which have been attributed to a flux-pinning effect. It should also be noticed that in a recent theoretical study of the superconducting-glass model,³³ which has been used to interpret the metastable properties of high- T_c materials, the same qualitative difference between the FC and ZFC magnetizations was found.

C. X-ray diffraction

The x-ray diffraction patterns indicate no detectable amounts of impurity phases ($< 1\%$) as Y_2BaCuO_5 , BaCuO_2 , or CoO . However, the cell parameters of the sample with $x = 0.05$ showed comparatively high standard deviations after the refinements. For this sample the diffraction lines are relatively broad which limits the accuracy of the line positions. The reason may be that an orthorhombic and a tetragonal form is coexisting or that the Co distribution in the material is inhomogeneous, or a combination of both effects. The changes in the lattice parameters and the unit-cell volume for different Co concentrations are presented in Fig. 4. The reported results

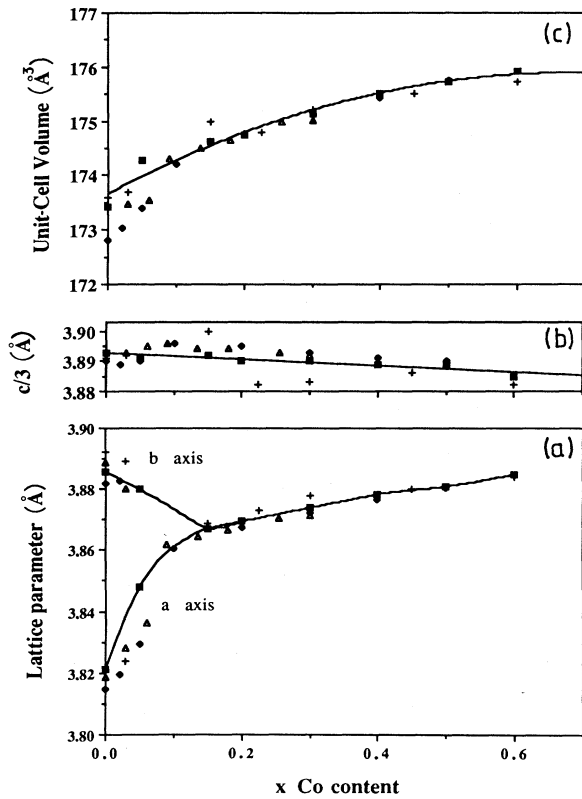


FIG. 4. Unit cell parameters (a, b, c, V) as a function of Co content in different samples of $\text{YBa}_2\text{Cu}_{3-x}\text{Co}_x\text{O}_{7-\delta}$. (■) present results; (Δ), (+), and (\blacklozenge) results of Refs. 32, 31, and 15, respectively. The lines are guides to the eye through the present results.

of other authors^{15,31,32} are also included in Fig. 4 for comparison. A summary of the lattice parameters is given in Table I, together with the T_c values obtained by resistivity and magnetic measurements. The immediate observation to be made from Fig. 4(a) is that the structure of $\text{YBa}_2\text{Cu}_{3-x}\text{Co}_x\text{O}_{7-\delta}$ transforms from orthorhombic to tetragonal for $0.05 < x < 0.15$. In the tetragonal phase the length of the a axis increases monotonically up

to the maximum concentration investigated. On the other hand, the c axis length decreases slightly with increasing Co concentration [see Fig. 4(b)]. The unit-cell volume increases throughout the investigated concentration range [see Fig. 4(c)].

D. Raman spectra

In Fig. 5 Raman spectra of fully oxygenated $\text{YBa}_2\text{Cu}_{3-x}\text{Co}_x\text{O}_{7-\delta}$ for $0 \leq x \leq 0.6$ are shown in the spectral region between 300 and 750 cm^{-1} , which is the typical region of the oxygen vibrations in the high- T_c superconductors. The Raman spectrum of the undoped Y-Ba-Cu-O is composed of three distinct peaks at 335 , 440 , and 502 cm^{-1} and a broad feature at frequencies $> 550 \text{ cm}^{-1}$. Recent reports on polarized Raman spectra from single crystals³⁴⁻³⁷ have unambiguously shown that the first three peaks are typical features of the superconducting phase. For increasing Co substitution we note several continuous changes in the spectra: (i) the intensity of the 335 cm^{-1} mode increases, (ii) the frequency of the 440 cm^{-1} mode increases, (iii) the frequency of the 502 cm^{-1} mode decreases, and (iv) the intensity of the broad band above 550 cm^{-1} increases. There is no sign of any abrupt change at the orthorhombic-to-tetragonal transition. All the spectra reside on a strong background which appears to be independent of the Co concentration. This background has been interpreted by several authors to be due to free-carrier scattering.^{22,23,30}

In Fig. 6 the peak frequencies of the 335 , 440 , and 502 cm^{-1} modes are presented as a function of Co concentration. Note the rapid decrease of the frequency of the 502 cm^{-1} mode with increasing x . For the samples with the largest Co concentration investigated the 502 cm^{-1} mode has decreased about 30 cm^{-1} compared to the undoped sample. The 440 cm^{-1} band increases only slightly and the frequency of the 335 cm^{-1} band appears to be constant with increasing x . The dependencies of the peak frequencies on Co concentration are reminiscent of the variations observed for decreasing oxygen content of the undoped Y-Ba-Cu-O.³⁸ The intensity variations of the 570 and 630 cm^{-1} bands with Co concentration are shown in Fig. 7. For small x the intensities of both modes increase rapidly while for larger x the intensities

TABLE I. Lengths of edges of the unit cell (a, b, c), the volume of the unit cell (V), and the midpoint superconducting critical temperatures, $T_c(R)$ and $T_c(F)$, derived from the resistivity and the FC magnetic transition curves, respectively, for $\text{YBa}_2\text{Cu}_{3-x}\text{Co}_x\text{O}_{7-\delta}$. Numbers in parentheses indicate the uncertainty of the last digit stated as one standard deviation.

x	a (Å)	b (Å)	c (Å)	V (Å ³)	$T_c(R)$ (K)	$T_c(F)$ (K)
0.00	3.8210(8)	3.8856(8)	11.680(4)	173.42	92	91
0.05	3.848(3)	3.880(3)	11.674(6)	174.28	90	89
0.15	3.8673(8)	3.8673(8)	11.675(3)	174.62	76	73
0.20	3.8695(4)	3.8695(4)	11.6709(9)	174.75	58	51
0.30	3.8740(2)	3.8740(2)	11.6696(7)	175.13	30	
0.40	3.8785(1)	3.8785(1)	11.6679(6)	175.51	4	
0.50	3.8810(3)	3.8810(3)	11.6663(9)	175.72	0	
0.60	3.8850(6)	3.8850(6)	11.655(2)	175.91	0	

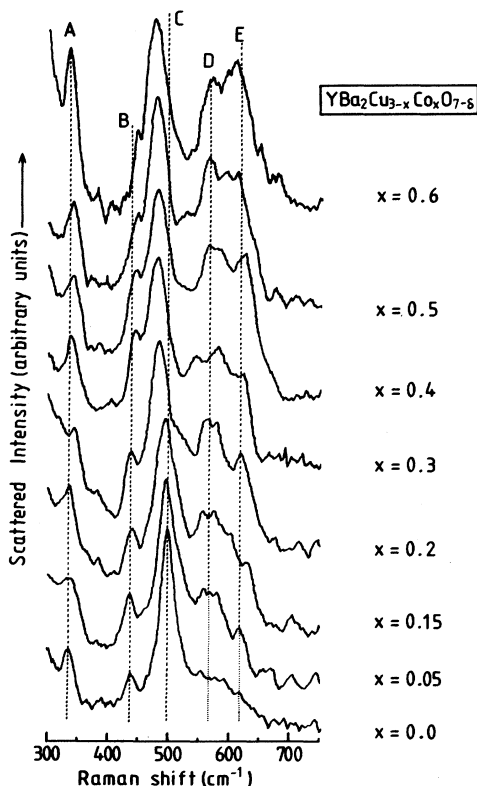


FIG. 5. Raman spectra of $\text{YBa}_2\text{Cu}_{3-x}\text{Co}_x\text{O}_{7-\delta}$ of different Co contents x in the range $300\text{--}750\text{ cm}^{-1}$.

seem to saturate at a constant level. All the changes in Fig. 6 and 7 of the peak frequencies and intensities are smooth without any observable discontinuities at the orthorhombic-to-tetragonal transition.

The 630 cm^{-1} mode shifts systematically to lower frequencies with increasing Co concentration and is observed at 620 cm^{-1} for the sample of maximum Co concentration investigated ($x=0.6$). However, the frequency of the 570 cm^{-1} band seems to be independent of Co concentration.

IV. DISCUSSION

A. Lattice parameters and T_c

The observation of an orthorhombic-to-tetragonal transition of $\text{YBa}_2\text{Cu}_{3-x}\text{Co}_x\text{O}_{7-\delta}$ for $0.05 < x < 0.15$ and the general behavior of the lattice parameters and T_c on the Co concentration are in agreement with results reported by other groups^{15,31,32} (see Figs. 3 and 4). The signatures of the orthorhombic-to-tetragonal transition for Co-substituted Y-Ba-Cu-O are different from those of the well-known oxygen-deficiency-induced orthorhombic-to-tetragonal transition of the undoped parent compound: (i) The superconductivity remains in the tetragonal phase as much larger Co concentrations than that inducing the orthorhombic-to-tetragonal transition, which is in contrast to the vanishing superconductivity close to the orthorhombic-to-tetragonal transition³⁹ in the case of ox-

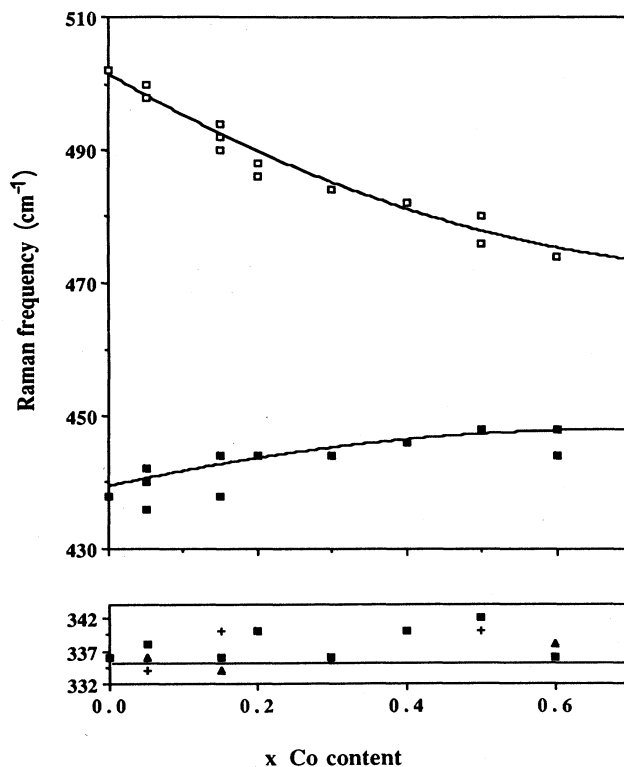


FIG. 6. The variation of the frequencies of the Raman modes at 335 , 440 , and 500 cm^{-1} as a function of Co content in $\text{YBa}_2\text{Cu}_{3-x}\text{Co}_x\text{O}_{7-\delta}$. The solid lines are guides to the eye.

xygen deficiency; (ii) the dependence of the a -axis length on Co substitution has an opposite trend compared to oxygen deficiency; (iii) the c -axis length increases markedly with decreasing oxygen content while it has a weak opposite dependence for increasing Co concentration.

Previously, it was suggested that high- T_c superconductivity and the orthorhombic structure are closely linked because of the nearly simultaneous orthorhombic-to-

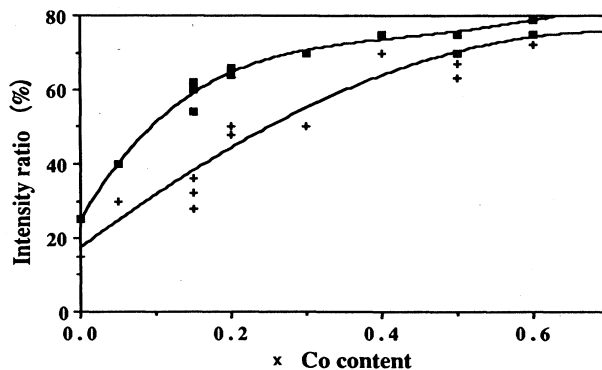


FIG. 7. Ratios of the peak heights of the 570 cm^{-1} (■) and 630 cm^{-1} (+) modes relative to the 500 cm^{-1} mode as a function of Co content in $\text{YBa}_2\text{Cu}_{3-x}\text{Co}_x\text{O}_{7-\delta}$. The solid lines are guides to the eye.

tetragonal transition and loss of superconductivity of Y-Ba-Cu-O for $\delta \approx 0.5$. However, the presence of high- T_c superconductivity in Co- and Fe-substituted Y-Ba-Cu-O (Ref. 15) and low-temperature oxidized pure Y-Ba-Cu-O samples of tetragonal structure³⁹ as well as the recent discovery of some Bi and Tl based high- T_c superconductors of tetragonal structure with even higher T_c (Ref. 40) has unambiguously shown that this suggestion is wrong.

It has been demonstrated by neutron-diffraction^{13–16} and EXAFS¹⁹ experiments that Co exclusively occupies the Cu(1) site. Since Co usually prefers an octahedral oxygen coordination stabilized by the Co^{3+} state it is expected that Co substitution on the Cu(1) site causes an introduction of extra oxygen atoms in the CuO chains. The Co substitution would then lead to an increasing oxygen occupation at the O(5) sites bridging the Cu(1)–O(1) chains. In fact the total oxygen content in Co-doped Y-Ba-Cu-O samples has been found to increase with increasing Co concentration^{15,31,41} to about $7 - \delta = 7.4$ for maximum Co concentration. The increase of the a -axis length in the tetragonal region and of the unit-cell volume with increasing Co concentration then reflect the higher coordination number of the Co ion and the extra oxygen brought into the structure. Miceli *et al.*¹⁴ have noted that one extra oxygen is introduced for every two Co in the a - b plane involving CuO chains and speculate that two Co form a local pair linked by an oxygen. Furthermore, they argue that the extra oxygen brought in by Co drives the orthorhombic-to-tetragonal transition by filling the O(5) sites adjacent to the chains. However, the tendency of Co to exist in octahedral coordinations and thereby cause a disordering of the CuO chains seems to be more important since the orthorhombic-to-tetragonal transition occurs for very small Co concentrations. This is supported by a recent EXAFS study¹⁹ of Co-substituted Y-Ba-Cu-O which shows that most of the Co(1) sites, and their neighboring oxygen sites are highly disordered. The authors suggest a model which would lead to a tetragonal structure; the Co atoms are displaced from the Cu(1) site and aggregate with extra oxygens into distorted zig-zag chains in the $\langle 110 \rangle$ directions. A similar displacement of the Co(1) sites has also been observed in a recent neutron-scattering study.⁴² The main changes of the local structure are expected to occur in the layer where the substitution takes place, i.e., in the CuO chains in case of Co doping. However, changes also occur in connection with the CuO_2 planes which are thought to be of prime importance for the superconductivity. The most evident changes of the local structure, as observed by neutron diffraction,^{14,42} are the shift of O(4) away from Cu(2) and the shift of Ba towards the CuO_2 plane. These changes are similar to those observed for a decrease of the oxygen content in unsubstituted Y-Ba-Cu-O.^{14,42,43} Therefore, the changes of the electron distribution around the CuO_2 plane seem to be similar in case of oxygen removal and Co substitution of the pure Y-Ba-Cu-O. Miceli *et al.*¹⁴ have noted identical correlation of T_c with the Cu(1)–O(4) bond length for oxygen deficient and Co-doped Y-Ba-Cu-O. However, the largest change is in the Cu(2)–O(4) distance which may be very sensitive to charge transfer between the CuO_2 planes and the CuO

chains and therefore also to the superconducting properties.

B. Phonon Raman spectra

1. Mode assignment

Recently, most of the phonon modes observed by Raman scattering from the undoped Y-Ba-Cu-O have been unambiguously assigned on the basis of single-crystal Raman experiments.^{34–37} Generally, five modes are observed around 116, 160, 335, 440, and 500 cm^{-1} , which are all assigned to vibrations in the c -axis direction. The 500 cm^{-1} mode is the Cu(1)–O(4)–Cu(2) stretching, the 440 cm^{-1} mode is the in-phase bending vibration of O(2), O(3) and the 335 cm^{-1} mode is the out-of-phase bending vibration of O(2), O(3). The 116 and 160 cm^{-1} modes, which are not observed in the present study owing to the large straylight background, are assigned to Ba and Cu(2) c -axis vibrations, respectively. We attribute the distinct Raman peaks observed for Co-substituted Y-Ba-Cu-O at 335, 440, and 500 cm^{-1} to the corresponding modes for pure Y-Ba-Cu-O. In pure Y-Ba-Cu-O additional modes have been observed at 220 cm^{-1} and in the region 550 – 650 cm^{-1} . In some reports^{34,37,44,45} these modes have been assigned to Raman-forbidden modes, which have become Raman active due to disorder induced by oxygen vacancies, defects, or twinning. A mode observed at 580 cm^{-1} has then been proposed to correspond to the ir-active Cu(1)–O(1) stretching vibration. In other reports^{46,47} the modes in the region 550 – 650 cm^{-1} have been attributed to impurities of BaCuO_2 , which have Raman modes at 636 and 576 cm^{-1} , and Y_2BaCuO_5 , which have a strong Raman mode at 600 cm^{-1} . A recent Raman study⁴⁸ of an untwinned single crystal of Y-Ba-Cu-O has shown the existence of disorder-induced modes at 580 and 220 cm^{-1} .

The disorder-induced modes related to the CuO chains should also become Raman active for Co-doped material because of the disorder introduced by the Co ions and the extra oxygens. A broad band in the region 550 – 650 cm^{-1} is present in the Raman spectrum of the Co-substituted Y-Ba-Cu-O (see Fig. 5). It consists of two main peaks at 570 and 630 cm^{-1} . The intensities of these modes increase considerably with increasing Co concentration, which suggests the assignment to disorder-induced modes. However, to be able to attribute the 570 and 630 cm^{-1} peaks to scattering from the superconducting Co-doped phase we need to exclude the possibility that they correspond to the nearly coincident BaCuO_2 modes at 576 and 636 cm^{-1} . The x-ray diffraction measurements did not reveal any detectable amount of impurities. Nevertheless, the modes can still be due to BaCuO_2 since the detection limit of the x-ray-diffraction measurements is of the order of 1% and the Raman scattering cross section of BaCuO_2 is much larger than for the superconducting phase. The intensity ratio of the 636 and 576 cm^{-1} peaks in pure BaCuO_2 is about 3 which is incompatible with our observation for the Co-doped Y-Ba-Cu-O samples and would seem to exclude the presence of BaCuO_2 . However, it has been reported

by Rosen *et al.*⁴⁷ that for small amounts of BaCuO₂ in Y-Ba-Cu-O both the absolute and relative intensities of the 636 and 576 cm⁻¹ modes of BaCuO₂ change dramatically with oxygen removal. A subsequent oxygen annealing recovered the original Raman features of BaCuO₂. A similar change of the Raman spectrum was observed for a sample of pure BaCuO₂ annealed at 950°C in air.⁴⁹ These results suggest that heat-treatment procedures can change the oxygen content of BaCuO₂ in a manner similar to that of Y-Ba-Cu-O. If a significant amount of such oxygen-deficient BaCuO₂ is present in our samples as impurity, a heat treatment under oxygen atmosphere should change the intensity patterns for the 570 and 630 cm⁻¹ bands. However, as demonstrated in Fig. 8 no significant change was observed in the Raman spectra of the original sample before and after annealing. Therefore we attribute the Raman features above 550 cm⁻¹ to disorder-induced Raman scattering rather than to contamination of BaCuO₂.

Moreover, the intensities of the 570 and 630 cm⁻¹ bands increase rapidly for small Co concentration but tend to saturate near $x=0.5$, which is the composition corresponding to the largest disorder in the CuO chains brought in by Co. A similar behavior has recently been reported^{44,45} for pure Y-Ba-Cu-O of different oxygen content, however restricted to the 570 cm⁻¹ peak. The behavior was attributed to the Cu(1)-O(1) stretching mode which was activated by an increasing disorder in the CuO chains caused by oxygen vacancies on the O(1) site.

The complex Raman band contour in the frequency region 550–650 cm⁻¹ of the Co-doped Y-Ba-Cu-O can be explained by possible overlapping of several Cu(1)-O(1) and Co(1)-O(1) modes of the heavily distorted chains with similar frequencies. The complexity is considerably enhanced for larger Co concentrations as shown in Fig. 5.

2. The effect of Co doping on the Raman phonon modes

The influence on the Raman spectrum of Y-Ba-Cu-O for Co substitution is similar to that for oxygen

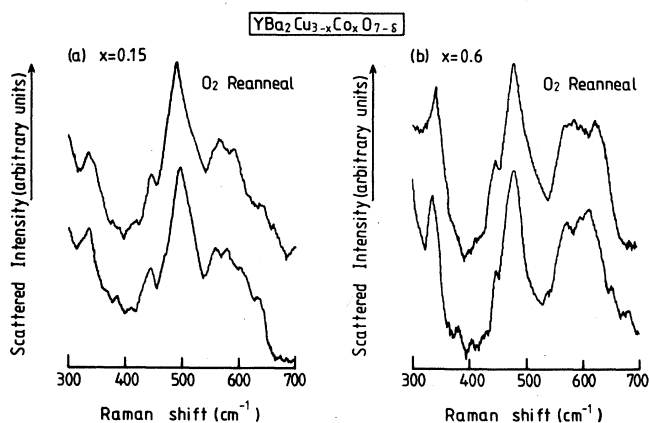


FIG. 8. Raman spectra of samples of YBa₂Cu_{3-x}Co_xO_{7-δ} with (a) $x=0.15$ and (b) $x=0.6$ before (lower trace) and after (upper trace) additional annealing at 400°C in oxygen.

deficiency; the intensity of the 335 cm⁻¹ mode increases, the frequency of the 440 cm⁻¹ mode increases slightly, the frequency of the 502 cm⁻¹ mode decreases considerably, and disorder-induced scattering around 570 cm⁻¹ increases with increasing Co concentration as well as for increasing oxygen deficiency.

The most prominent change in the Raman spectra for both Co doping and oxygen deficiency is the decreasing frequency of the 502 cm⁻¹ mode [O(4) axial stretch]. Several attempts have been made to correlate this mode and its corresponding ir antisymmetric stretching mode at 573 cm⁻¹ (Ref. 50) to either the c -axis length or the Cu(1)-O(4) distance which is by far the shortest Cu-O distance in Y-Ba-Cu-O. The frequency dependence seems to be well correlated with the increase of the c -axis length for decreasing oxygen content.⁵¹ However, in the case of Co substitution the c -axis length behaves oppositely, it decreases weakly with increasing cobalt content, which rules out the c -axis length to be the important factor for the changes of the O(4) stretching vibrational frequency. It seems plausible that the O(4) stretching mode would mainly be determined by the Cu(1)-O(4) force constant since this distance is much shorter than the Cu(2)-O(4) distance. Interestingly, the Cu(1)-O(4) distance decreases for increasing cobalt concentration as well as for increasing oxygen deficiency. The vibrational frequency is then expected to increase (as a result of an increase of the force constant), which is the opposite behavior to that observed in the present study and to that observed for oxygen deficiency.^{38,44,45,52} For a simple oscillator the frequency is expected to depend on the distance d as $\omega \sim d^{-4}$. The decrease of the Cu(1)-O(4) distance of 0.025 Å for either a Co concentration of $x=0.4$ (Ref. 14) or an oxygen deficiency of $\delta \approx 0.5$ (Ref. 43) is then expected to give a 30 cm⁻¹ higher frequency of the O(4) stretching mode compared to the pure fully oxygenated compound. Instead a downward shift of about the same magnitude is observed in the present study as well as for the case of oxygen deficiency.^{38,44,45,52} If the Cu(2)-O(4) distance, which increases when the Cu(1)-O(4) distance decreases, is taken into account the discrepancy between the O(4) oxygen stretching frequency and the bond lengths will only partly be compensated.

What is then the origin of the downshift of the O(4) stretching mode for increasing Co content or oxygen deficiency? It has been argued that a change of the charge distribution and of the orbitals around Cu(1) can explain the behavior of the frequency shift for oxygen-deficient samples. However, it seems rather unlikely that a change of the Cu(1) orbitals simultaneously binds the O(4) closer to the CuO chains and cause a decrease of the Cu(1)-O(4) force constant (i.e., a negative frequency shift). Recently, it has been proposed that the frequency of the 500 cm⁻¹ mode is directly proportional to the hole concentration and thus to T_c for pure Y-Ba-Cu-O of varying oxygen content.⁵³ In order to test this assumption we have plotted T_c versus the frequency of the 500 cm⁻¹ mode in Fig. 9 for the present Co-substituted samples and also for the case of oxygen-deficient samples.^{38,52} As seen in Fig. 9 the correlation between T_c and the O(4) stretching frequency is remarkably similar for Co substitution

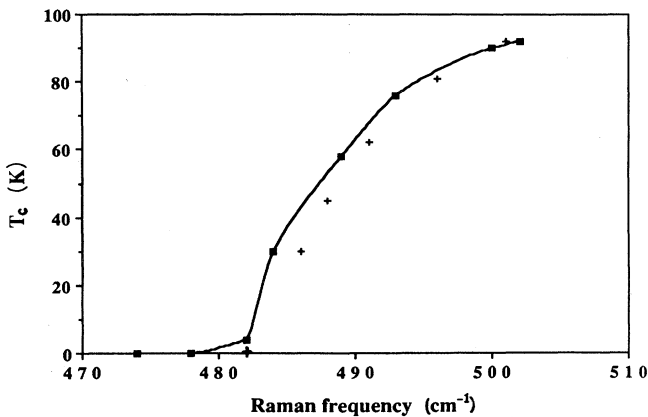


FIG. 9. Plot of T_c vs the frequency of the O(4) axial stretching vibration for (■) Co substitution and (+) oxygen deficiency (Refs. 38 and 52). The solid line is a guide to the eye.

and oxygen deficiency of Y-Ba-Cu-O. It is tempting to ascribe the changes of the O(4) stretching frequency to the number of free holes since it is well established that T_c of the cuprate superconductors is directly proportional to the hole concentration.⁵⁴ The decreasing frequency of the O(4) vibration is then explained by a decrease of the attractive force between $(\text{Cu-O})^+$ holes in the CuO_2 planes and the negative charge of O(4). Interestingly, the Ba ion comes closer to the CuO_2 plane for both oxygen deficiency and increasing Co concentration,^{14,42} which is then consistent with the proposed picture of a decreasing positive charge $(\text{Cu-O})^+$ in the CuO_2 planes. However, since the oxygen concentration for Co-substituted samples is generally higher than 7, one oxygen is introduced for every two Co^{3+} in the CuO chains, the formal valence of Cu or O is essentially unchanged which would mean, in principle, that the total-hole concentration is unchanged. In contrast to this assumption recent Hall effect measurements⁵⁵ have shown that the number of free carriers decreases with increasing Co concentration. This then lends support to the suggestion that the charge carrier concentration is directly reflected in the frequency of the O(4) axial stretching vibration.⁵³ Nevertheless, it seems natural that the frequency of the O(4) vibration is very sensitive to the charge balance or charge fluctuations between the chains and the planes since the O(4)s are the charge links between the chains and planes. This balance has been proposed to be of vital importance for the superconducting properties since the chains (or the intercalated Tl and Bi layers in case of Bi and Tl based superconductors) act as charge reservoirs and provide the hole-charge carriers for the planes in which the superconductivity takes place.⁵⁶ Recently, Tokura *et al.*⁵⁷ have tried to estimate how the holes associated with the $(\text{Cu-O})^+$ charge are distributed between the CuO_2 planes and the CuO chains based on their data for many samples in the $(\text{Ca}_x\text{Y}_{1-x})\text{Ba}_2\text{Cu}_3\text{O}_y$ and $\text{Y}(\text{La}_x\text{Ba}_{1-x})_2\text{Cu}_3\text{O}_y$ systems where both the oxygen content and the average Cu valence can be separately varied over a wide range. They have concluded that the holes localized within the CuO chains merely provide an insulating reservoir of charge

and that the number of the mobile holes on the CuO_2 planes rather than the total-hole concentration is the essential variable governing the superconducting properties. According to the idea of Tokura *et al.*⁵⁷ together with consideration for both the observed increase in the oxygen content^{15,31,41} and the reported strong decrease in the Hall number⁵⁵ with increasing Co concentration, which in the former suggests constancy of total-hole concentration, while in the latter would be directly related to the decreasing number of mobile holes on the CuO_2 planes, it can be speculated that the hole population between the CuO_2 planes and the CuO chains is significantly altered for increasing Co content. We thus expect that an increasing number of holes becomes localized within the CuO chains, while the decrease in the hole concentration on the CuO_2 planes, with which we correlate the downshift of the 500 cm^{-1} O(4) stretching mode for increasing Co content or oxygen deficiency, results in an eventual decrease in T_c .

V. CONCLUSION

The effect of Co substitution for Cu in $\text{YBa}_2\text{Cu}_{3-x}\text{Co}_x\text{O}_{7-\delta}$ on the superconducting properties, the structure and the Raman active vibrational modes have been investigated for Co contents in the range $0 \leq x \leq 0.6$. T_c is observed to decrease linearly with increasing Co content for $x > 0.1$ and vanishes around $x = 0.4$. An orthorhombic-to-tetragonal phase transition is observed around $x = 0.15$, i.e., the superconductivity remains well into the concentration region of the tetragonal phase.

The observed changes of the Raman spectra with increasing Co concentration are reminiscent of those reported for increasing oxygen deficiency, despite that the lattice parameters show different behavior for Co substitution and oxygen deficiency. Changes in the Raman spectra are related to local valence, bond lengths, and charge-transfer changes, which can affect the interaction that may be important. Interestingly, the frequencies of the O(4) axial stretching vibration at around 500 cm^{-1} , which has been proposed to be proportional to the free-charge carrier concentration, exhibit large downward shifts for increasing Co concentration as well as for increasing oxygen deficiency. In fact, the same linear dependence of T_c on the frequency of the O(4) axial stretching vibration is found for both Co substitution and oxygen deficiency. The present results then indicate that the oxygen vibrational modes as well as T_c are sensitive to local changes of the valency and the charge balance between the chains and the planes and that the O(4)s play an essential role for charge transfer between the CuO chains and the CuO_2 planes. It is suggested that an increasing number of $(\text{Cu-O})^+$ holes becomes localized within the chains and therefore does not contribute to the superconductivity which occurs in the CuO_2 planes. Thus, the decrease of T_c for increasing Co substitution as well as for increasing oxygen deficiency is explained by a decreasing number of free-charge carriers in the CuO_2 planes.

The introduction of Co^{3+} ions at the Cu(1) sites causes

a distortion of the CuO chains which is observed as an increase of the intensity of a Raman-forbidden broad band around 570 cm^{-1} . This band is assigned to the ir-active and Raman-forbidden Cu(1)-O(1) stretching mode of the pure perfect crystal of Y-Ba-Cu-O, which has become Raman active by the disorder introduced in the chains by the Co ions.

ACKNOWLEDGMENTS

The authors are grateful to Professor T. Claeson for providing results prior to publication. This work was financially supported by the Swedish Natural Science Research Council.

- ¹J. G. Bednorz and K. A. Müller, *Z. Phys. B* **64**, 189 (1986).
- ²C. W. Chu, P. H. Hor, R. L. Meng, L. Gao, Z. J. Huang, and Y. Q. Wang, *Phys. Rev. Lett.* **58**, 405 (1987).
- ³(a) V. J. Emery, *Phys. Rev. Lett.* **58**, 2794 (1987); A. Aharony, R. J. Birgeneau, A. Coniglio, M. A. Kastner, and H. E. Stanley, *ibid.* **60**, 1330 (1988); V. J. Emery, *Mater. Res. Bull.* **14**, 67 (1989); J. R. Schrieffer, X. G. Wen, and S. C. Zhang, *Phys. Rev. Lett.* **60**, 944 (1988); (b) C. M. Varma, S. Schmitt-Rink, and E. Abrahams, *Solid State Commun.* **62**, 681 (1987); (c) R. Zeyer and G. Zwirnagel, *ibid.* **66**, 617 (1988); (d) J. C. Phillips, *ibid.* **65**, 227 (1988); (e) P. W. Anderson, *Science* **235**, 1196 (1987).
- ⁴For a recent review of the different models see, for example, P. Fulde, *Phys. Scr. T* **23**, 101 (1988).
- ⁵B. T. Matthias, H. Sohl, and E. Corenzwit, *Phys. Rev. Lett.* **1**, 93 (1958).
- ⁶A. A. Abrikosov and L. P. Gorkov, *Zh. Eksp. Teor. Fiz.* **39**, 1781 (1960) [*Sov. Phys.—JETP* **12**, 1243 (1960)].
- ⁷J. M. Tarascon, W. R. McKinnon, L. H. Greene, G. W. Hull, and E. M. Vogel, *Phys. Rev. B* **36**, 226 (1987); D. W. Murphy, S. Sunshine, R. B. van Dover, R. J. Cava, B. Batlogg, S. M. Zuharak, and L. F. Schneemeyer, *Phys. Rev. Lett.* **58**, 1888 (1987); P. H. Hor, R. L. Meng, Y. Q. Wang, L. Gao, Z. J. Huang, J. Bechtold, K. Forster, and C. W. Chu, *ibid.* **58**, 1891 (1987); T. J. Kistenmacher, *Solid State Commun.* **65**, 981 (1988).
- ⁸B. W. Veal, W. K. Kwok, A. Umezawa, G. N. Crabtree, J. D. Jorgensen, J. W. Downey, L. J. Nowicki, A. W. Mitchell, A. P. Paulikas, and C. H. Sowers, *Appl. Phys. Lett.* **51**, 279 (1987); A. Ono, T. Tanaka, H. Nozaki, and Y. Ishizawa, *Jpn. J. Appl. Phys.* **26**, L1687 (1987); T. Wada, S. Adachi, O. Inoue, S. Kawashima, and T. Mihara, *ibid.* **26**, L1475 (1987).
- ⁹S. B. Oseroff, D. C. Vier, J. F. Smyth, C. T. Salling, S. Schultz, Y. Dalichaouch, B. W. Lee, M. B. Maple, Z. Fisk, J. D. Thompson, J. L. Smith, and E. Zirngiebl, *Solid State Commun.* **64**, 241 (1987).
- ¹⁰P. Strobel, C. Paulsen, and J. L. Tholence, *Solid State Commun.* **65**, 585 (1988).
- ¹¹M. F. Yan, W. W. Rhodes, and P. K. Gallagher, *J. Appl. Phys.* **63**, 821 (1988).
- ¹²G. Xiao, F. H. Streitz, A. Gavrin, M. Z. Cieplak, C. L. Chien, and A. Bakhshai, *J. Appl. Phys.* **63**, 4196 (1988).
- ¹³T. Kajitani, K. Kusaba, M. Kikuchi, Y. Syono, and M. Hirabayashi, *Jpn. J. Appl. Phys.* **26**, L1727 (1987); **27**, L354 (1988).
- ¹⁴P. F. Miceli, J. M. Tarascon, L. H. Greene, P. Barboux, F. J. Rotella, and J. D. Jorgensen, *Phys. Rev. B* **37**, 5932 (1988).
- ¹⁵J. M. Tarascon, P. Barboux, P. F. Miceli, L. H. Greene, G. W. Hull, M. Eibschutz, and S. A. Sunshine, *Phys. Rev. B* **37**, 7458 (1988).
- ¹⁶G. Roth, G. Heger, B. Renker, J. Pannetier, V. Caignaert, M. Hervieu, and B. Raveau, *Z. Phys. B* **71**, 43 (1988).
- ¹⁷T. Tamaki, K. Komai, A. Ito, Y. Maeno, and T. Fujita, *Solid State Commun.* **65**, 43 (1988).
- ¹⁸S. Nasu, H. Kitagawa, Y. Oda, T. Kohara, T. Shinjo, K. Asayama, and F. E. Fujita, *Physica* **148B**, 484 (1987).
- ¹⁹F. Bridges, J. B. Boyce, T. Claeson, T. H. Geballe, and J. M. Tarascon, *Phys. Rev. B* **39**, 11 603 (1989).
- ²⁰T. J. Kistenmacher, *Phys. Rev. B* **38**, 8862 (1988).
- ²¹P. F. Miceli, J. M. Tarascon, L. H. Greene, P. Barboux, M. Giroud, D. A. Neumann, J. J. Rhyne, L. F. Schneemeyer, and J. V. Waszczak, *Phys. Rev. B* **38**, 9209 (1988).
- ²²For an excellent, recent review of Raman scattering from high- T_c superconductors, see C. Thomsen and M. Cardona, in *Physical Properties of High-Temperature Superconductors*, edited by D. M. Ginsberg (World Scientific, Singapore, 1989).
- ²³S. L. Cooper, M. V. Klein, B. G. Pazol, J. P. Rice, and D. M. Ginsberg, *Phys. Rev. B* **37**, 5920 (1988).
- ²⁴M. Krantz, H. J. Rosen, R. M. MacFarlane, and V. Y. Lee, *Phys. Rev. B* **38**, 4992 (1988).
- ²⁵A. Witlin, R. Lin, M. Cardona, L. Gonzel, W. König, W. Bauhofer, H. Mattausch, and A. Simon, *Solid State Commun.* **64**, 477 (1987).
- ²⁶R. Feile, P. Leidere, J. Kowalewski, W. Assmus, J. Schubert, and U. Poppe, *Z. Phys.* **73B**, 155 (1988).
- ²⁷K. B. Lyons, P. A. Fleury, L. F. Schneemeyer, and J. V. Waszczak, *Phys. Rev. Lett.* **60**, 732 (1988).
- ²⁸S. Sugai, S. Shamoto, and M. Sabo, *Phys. Rev. B* **38**, 6436 (1988).
- ²⁹S. Sugai, Proceedings of the Second NEC Symposium on Fundamental Approach to New Materials Phases, Japan, 1988, (unpublished).
- ³⁰D. M. Krol, M. Stavola, L. F. Schneemeyer, J. V. Waszczak, H. O'Bryan, and S. A. Sunshine, *Phys. Rev. B* **38**, 11 346 (1988).
- ³¹J. F. Bringley, T. M. Chen, B. A. Averill, K. M. Wong, and S. J. Poon, *Phys. Rev. B* **38**, 2432 (1988).
- ³²Y. Maeno and T. Fujita, *Physica* **153-155C**, 1105 (1988).
- ³³J. Choi and J. V. José, *Phys. Rev. Lett.* **62**, 320 (1989).
- ³⁴D. M. Krol, M. Stavola, W. Weber, L. F. Schneemeyer, J. V. Waszczak, S. M. Zahurak, and S. G. Kosinski, *Phys. Rev. B* **36**, 8325 (1987).
- ³⁵A. Yamanaka, F. Minami, K. Watanabe, K. Inoue, S. Takekawa, and N. Iyi, *Jpn. J. Appl. Phys.* **26**, L1404 (1987).
- ³⁶V. G. Hadjiev and M. N. Iliev, *Solid State Commun.* **66**, 451 (1988).
- ³⁷R. Liu, C. Thomsen, W. Kress, M. Cardona, B. Gegenheimer, F. W. de Wette, J. Prade, A. D. Kulkarni, and U. Schröder, *Phys. Rev. B* **37**, 7971 (1988).
- ³⁸C. Thomsen, R. Liu, M. Bauer, A. Wittlin, L. Genzel, M. Cardona, E. Schönher, W. Bauhofer, and W. König, *Solid State Commun.* **65**, 55 (1988); S. Sugai, *Phys. Rev. B* **36**, 7133 (1987); R. M. Macfarlane, H. J. Rosen, E. M. Engler, R. D. Jacowitz, and V. Y. Lee, *ibid.* **38**, 284 (1988).
- ³⁹R. J. Cava, B. Batlogg, S. A. Sunshine, T. Siegrist, R. M. Fleming, K. Rabe, L. F. Schneemeyer, D. W. Murphy, R. B. van Dover, P. K. Gallagher, S. H. Glarum, S. Nakahara, R.

- C. Farrow, J. J. Krajewski, S. M. Zahurak, J. V. Waszczak, J. H. Marshall, P. Marsch, L. W. Rupp, W. F. Peck, and E. A. Rietman, *Physica* **153-155C**, 560 (1988).
- ⁴⁰R. M. Hazen, C. T. Prewitt, R. J. Angel, N. L. Ross, L. W. Finger, C. G. Hadidiacos, D. R. Veblen, P. J. Heaney, P. H. Hor, R. L. Meng, Y. Y. Sun, Y. Q. Wang, Y. Y. Xue, X. J. Huang, L. Gao, J. Bechtold, and C. W. Chu, *Phys. Rev. Lett.* **60**, 1174 (1988); Z. Z. Sheng, A. M. Hermann, A. EiAli, C. Almasan, J. Estrada, T. Datta, and R. J. Matson, *ibid.* **60**, 937 (1988).
- ⁴¹Y. K. Tao, J. S. Swinnea, A. Manthiram, J. S. Kim, J. B. Goodenough, and H. Steinfink, *J. Mater. Res.* **3**, 248 (1988).
- ⁴²P. Zolliker, D. E. Cox, J. M. Tranquada, and G. Shirane, *Phys. Rev. B* **38**, 6575 (1988).
- ⁴³W. K. Kwok, G. W. Crabtree, A. Umezawa, B. W. Veal, J. D. Jorgensen, S. K. Malik, L. J. Nowicki, A. P. Paulikas, and L. Nunez, *Phys. Rev. B* **37**, 106 (1988).
- ⁴⁴K. F. McCarty, J. C. Hamilton, R. N. Shelton, and D. S. Ginley, *Phys. Rev. B* **38**, 2914 (1988).
- ⁴⁵R. Nishitani, N. Yoshida, Y. Sasaki, and Y. Nishina, *Jpn. J. Appl. Phys.* **27**, L1284 (1988).
- ⁴⁶R. Bhadra, T. O. Brun, M. A. Beno, B. Dabrowski, D. G. Hinks, J. Z. Liu, J. D. Jorgensen, L. J. Nowicki, A. P. Paulikas, I. K. Schuller, C. U. Segre, L. Soderholm, B. Veal, H. H. Wang, J. M. Williams, K. Zhang, and M. Grimsditch, *Phys. Rev. B* **37**, 5142 (1988).
- ⁴⁷H. J. Rosen, R. M. Macfarlane, E. M. Engler, V. Y. Lee, and R. D. Jacowitz, *Phys. Rev. B* **38**, 2460 (1988); R. M. Macfarlane, H. J. Rosen, E. M. Engler, R. D. Jacowitz, and V. Y. Lee, *ibid.* **38**, 284 (1988).
- ⁴⁸C. Thomsen, M. Cardona, B. Gegenheimer, R. Liu, and A. Simon, *Phys. Rev. B* **37**, 9860 (1988).
- ⁴⁹M. Kakihana, L. Börjesson, L. M. Torell, Z. Liu, and S. G. Eriksson, *Physica* **156C**, 420 (1988).
- ⁵⁰G. Ruani, C. Taliani, R. Zamboni, D. Cittone, and F. C. Matocotta, *J. Opt. Soc. Am. B* **6**, 409 (1989).
- ⁵¹A. Manthiram, J. S. Swinnea, Z. T. Sui, H. Steinfink, and J. B. Goodenough, *J. Am. Chem. Soc.* **109**, 6667 (1987); R. Meuffels, B. Rupp, and E. Pörschke, *Physica* **156C**, 441 (1988); W. Wong-Ng, L. P. Cook, C. K. Chiang, L. J. Swartzendruber, L. H. Bennett, J. Blendell and D. Minor, *J. Mater. Res.* **3**, 832 (1988).
- ⁵²M. Hangyo, S. Nakashima, K. Mizoguchi, A. Fujii, A. Mitsuishi, and T. Yotsuya, *Solid State Commun.* **65**, 835 (1988).
- ⁵³V. M. Agranovich, V. N. Denisov, V. E. Krautsov, B. N. Mavrin, and V. B. Podobedov, *Phys. Lett.* **134A**, 186 (1988).
- ⁵⁴P. Steiner, S. Hufner, V. Kinsinger, I. Sander, B. Siegwart, H. Schmitt, R. Schulz, S. Junk, G. Schwitzgebel, A. Gold, C. Politis, H. P. Müller, R. Hoppe, S. Keemler-Sack, and C. Kunz, *Z. Phys. B* **69**, 449 (1988).
- ⁵⁵J. Clayhold, S. Hagen, Z. Z. Wang, N. P. Ong, J. M. Tarascon, and P. Barboux, *Phys. Rev. B* **39**, 777 (1989).
- ⁵⁶J. M. Tarascon and B. G. Bagley, *Mater. Res. Bull.* **14**, 53 (1989).
- ⁵⁷Y. Tokura, J. B. Torrance, T. C. Huang, and A. I. Nazzal, *Phys. Rev. B* **38**, 7156 (1988).